Modular Nanocomposite Films with Tunable Physical Organization of Cellulose Nanocrystals for Photonic Encryption

Yang Yang, Xiaojie Wang, Heqin Huang, Shiqiang Cui, Ye Chen, Xiaohui Wang,* and Kai Zhang*

Reported herein is the novel achievement of uniform and tunable interference colors of nanocomposite films containing organized cellulose nanocrystals (CNCs) from dynamic hydrogel precursors. Homogeneous and amendable interference colors with broad range are obtained either by stacking the nanocomposite films to adjust the amount of CNCs in the propagation pathway of light or by regulating the rotation angles between the individual films to alter the relative organization of CNCs within the system. Moreover, the precise and controllable patterned CNC composite films with multicolors in one film are facilely fabricated for the first time from the patterned hydrogel precursors. Based on this stacking/rotation-method, these patterned nanocomposite films with tunable interference colors can be further applied as fundamental elements for optical encryption by establishing a ternary-coded decimal system with encoded decimal numerals, paving the way for the development of photonic functional materials based on CNCs.

Photonic materials can manipulate light by prohibiting propagation of certain wavelengths, thus generating structure colors and optical properties for photonic applications including sensors, actuators, security labeling, encryption, anticounterfeiting, and so on.[1,2] Diverse photonic structures have been reported, such as photonic crystals and Bragg stacks.[3,4] Generally, the iridescent colors produced by photonic crystals or Bragg stacks can be altered by changing either the particles' size, the spacing among particles in photonic crystals, or the thickness of overlapped layers in a Bragg stack in response to a stimulus.[5]

Among them, chiral nematic liquid crystals with the ability to self-assembly into helical structures can selectively reflect the incident light.[4,6] Typically, cellulose nanocrystals (CNCs), derived from biomass via sulfuric acid hydrolysis or 2,2,6,6-tetramethylpiperidinyloxy (TEMPO)-mediated oxidation, possess the intriguing ability to self-assembly into a chiral nematic liquid crystals phase in sufficiently concentrated solutions.[7,8] Aqueous CNCs suspensions can be turned into iridescent solid films with a left-handed helical structure upon air-drying. The reflected light with certain wavelengths by solid CNCs films could be controlled by changing the helical pitch in suspensions via introducing electrolytes, varying the evaporation rate and substrates, coassembly of CNCs with polymeric networks, applying sonication, mechanical shearing, electrical or magnetic field.[9–11]

In order to use the photonic properties of CNCs, many efforts have been devoted during the past few years to developing the uniform long-range helical order and homogeneous structure color by manipulating the pitch size and the chiral nematic organization in solid CNCs films. Various nanocomposite hydrogels,[4] films,[11] and elastomer[8] have been prepared in previous studies by evaporation-induced self-assembly (EISA) of CNCs together with various polymers. However, the procedures of EISA are highly sensitive, sophisticated and often require long time to concentrate a CNCs suspension to the desired concentration of above 10 wt%. In addition, various techniques, such as electromagnetic field and circular shear flow, also proved to facilitate chiral nematic alignment and improve the uniformity in helix orientation.[10,12] Despite these advances, most of color changes can only be realized in aqueous suspensions via the alteration of the pitch sizes of helical structures, which also limit their applications as solid optical

Dr. Y. Yang, Prof. X. Wang
State Key Laboratory of Pulp and Paper Engineering
South China University of Technology
Guangzhou 510640, P. R. China
E-mail: fewangxh@scut.edu.cn
Dr. Y. Yang, X. Wang, Dr. H. Huang, Prof. K. Zhang
Wood Technology and Wood Chemistry
Department of Wood Technology and Wood-Based Composites
University of Goettingen
Büsgenweg 4, Göttingen D-37077, Germany
E-mail: kai.zhang@uni-goettingen.de
S. Cui, Prof. Y. Chen
State Key Laboratory for Modification of Chemical Fibers and Polymer Materials
College of Materials Science and Engineering
Donghua University
Shanghai 201620, P. R. China

The ORCID identification number(s) for the author(s) of this article can be found under https://doi.org/10.1002/adom.202000547.

components. It is still highly challenging to use CNCs for the fabrication of photonic materials with homogeneous color for photonic applications, in particular because of the lack of a continuous, modularly implementable and efficient technique for the adjustment of the interference colors in a broad range.

In addition to the achievement of single uniform interference color, the incorporation of multiple interference colors as individual bordering patterns is a further challenge. Only a few studies reported the production of photonic patterns in CNC-based films, e.g., by using heat to produce areas with different thickness,[13] differential evaporation to regions,[14] solvent-assisted soft nanoimprint lithography,[15] using diverse solvents as inks[16] or by forming a CNCs film with gradient color through masked evaporation.[17] However, the patterns in these CNCs films showed the relatively low resolution with limited colors, and the processes were also extremely hard to control. These drawbacks limited the application of patterned CNCs films in optical encoding and encryption of information, so that

still no report about precise and effectively useful coding based on the patterned CNCs films is known up to now.

Herein, we developed a novel and cost-efficient approach to tune the uniform interference colors by stacking the nanocomposite films in piles. These nanocomposite films with aligned CNCs can be modularly piled with desired rotation angles to adjust the final colors owing to the rotated directions of CNCs relative to each other. To the best of our knowledge, it is the first time to realize the patterned CNC-based nanocomposite films with clear boundaries of various facilely adjustable and uniform interference colors. These modular nanocomposite films further showed their potential for various applications as photonic materials, such as for encryption of information.

The detailed process for the preparation of composite films containing CNCs was schematically illustrated in **Figure 1**a. In the first step, the composite films with highly ordered CNCs were prepared via the mechanical stretching and air-drying of dynamic hydrogels with polyacrylamide (PAM) as matrix that
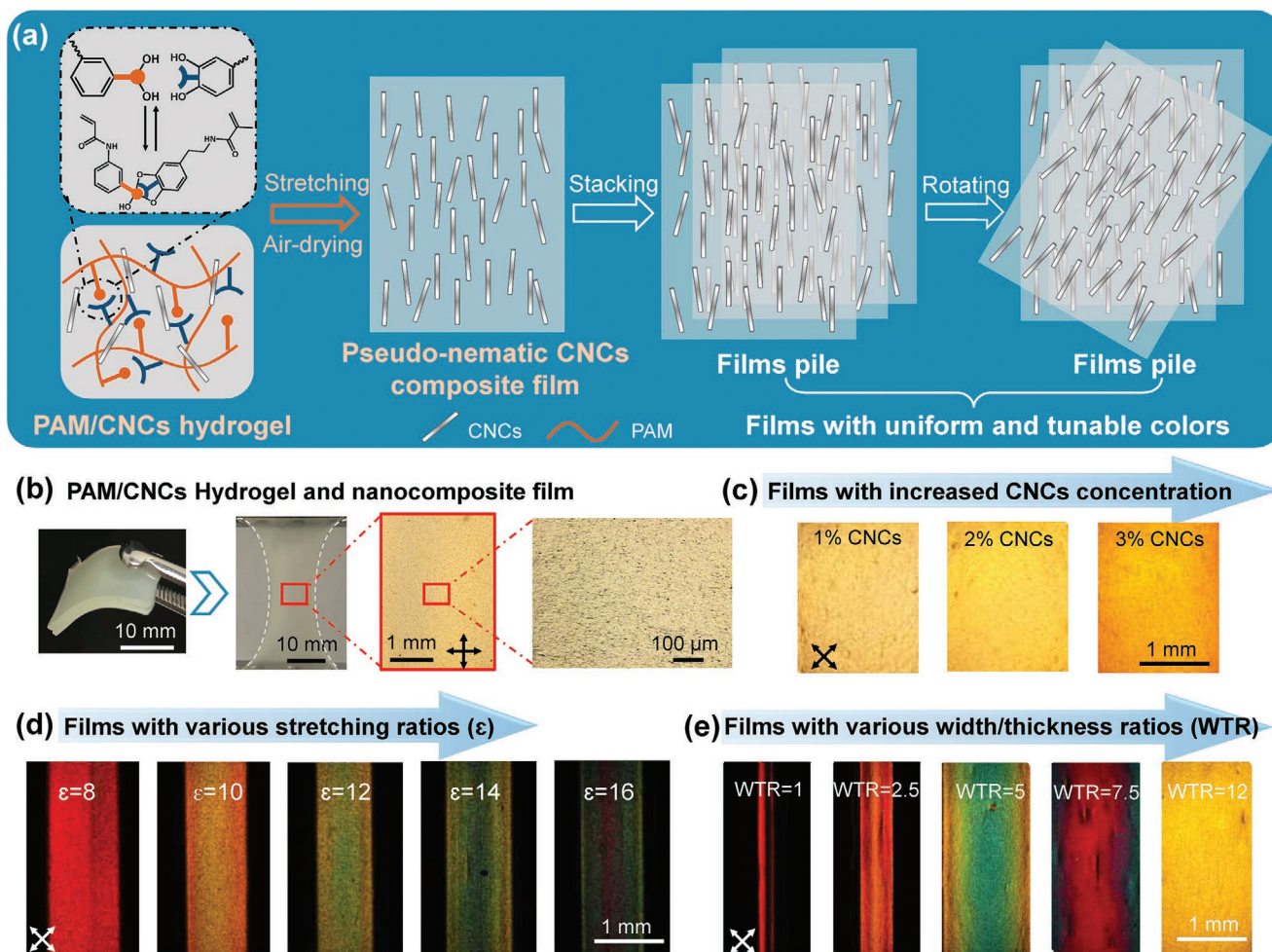

Figure 1. Fabrication of CNCs composite films with uniform and tunable interference colors. a) Schematic illustration for the two-step approach for the preparation of photonic CNCs composite films with uniform and tunable colors: (1) preparation of single CNCs composite films via the hydrodynamic alignment of CNCs in the dynamic hydrogels under stretching and further confined assembly during air-drying process. (2) Color manipulation by stacking and rotating the CNCs composite films in piles. b) Photos of the as-prepared hydrogels crosslinked using dynamic covalent bonds and the film after stretching and air-drying. The POM image shows the uniform color of the middle area of the composite film. The laser scanning microscope image exhibits the smooth surface of the composite film. c–e) POM images of the CNCs composite films with various concentrations of c) CNCs, d) stretching ratios (ε), and e) width/thickness ratios (WTR).

**ADVANCED
SCIENCE NEWS**
www.advancedsciencenews.com

**ADVANCED
OPTICAL
MATERIALS**
www.advopticalmat.de

was crosslinked via dynamic covalent bonds formed by dopamine methylacrylate (DMA)/3-(acrylamido) phenylboronic acid (PBAAm).[18,19] In the second step, the arrangement of CNCs in the multilayer material system was tuned by stacking the CNCs composite films in piles and regulating the rotation angles between them, resulting in the composite films with vivid and tunable interference colors.

To be precise, the dynamic hydrogels were prepared by in situ polymerization of acrylamide in the basic buffer with phenylboronic acid/catechol complexes as dynamic crosslinkers in the presence of anisotropic CNCs (Figure 1a and Figure S1, Supporting Information). The monoborate ions reacted with cis–diol to form dynamic borate ester complexes. Different from the traditional EISA of CNCs films, mechanical stretching was used to prealign CNCs in the hydrogels. These dynamic hydrogels exhibited elastoplastic behaviors during the uniaxial stretching.[18] During the following air-drying process, the surface tension further enhanced the orientation of CNCs in the confined geometry, leading to composite films containing CNCs as illustrated in Figure 1a. The anisotropic CNCs used here were prepared via TEMPO-mediated oxidation according to previous report.[18] They had diameters ≈10 nm and lengths of 100–200 nm. In addition, these CNCs contain carboxyl groups of 1.50 ± 0.02 mmol g^{-1} and aldehyde groups of 0.12 ± 0.02 mmol g^{-1} on the surface, giving rise to their good dispersion in neutral or weak basic aqueous solutions. The loading amount of CNCs in the hydrogels was tuned between 0 and 3 wt%. After the preparation of the dynamic hydrogels, they were further stretched and dried in air for films (Figure 1b). The surface of obtained composite films was generally very smooth with root-mean-square roughness (Rq) of 1.33 μm, according to the laser scanning microscopic (LSM) analysis (Figure 1b and Figure S2, Supporting Information). Such flat composite films generally had high transparency of up to 70% in the wavelength range of visible light (Figure S3, Supporting Information). The transparency of films decreased with the increasing thickness of the original hydrogels and therefore resulting films. Different from other strain-induced alignment of CNCs in elastic polymer matrix, the aligned CNCs were stabilized in the relaxed polymer matrix due to the much faster relaxation of polymer networks than CNCs after unloading the external force, as reported in our previous work.[18] In particular, these relaxed PAM chains will not generate any interference color, so that only aligned CNCs within the polymeric matrix are the sources for it. It should be noted that the vivid interference colors shown by composite films were only visible between the crossed polarizers (Figure 1b). Compared to other studies, the uniform and tunable interference colors presented by the composite films are only based on the physically organized CNCs, without any interference of aligned polymer chains or stressed matrix. Thus, the interference colors we observed are only attributed to the light retardation caused by the oriented CNCs. These interference colors reached the maximum intensity with the stretching direction fixed at 45° against polarizers. The incident light was completely blocked, when the stretching direction was parallel or perpendicular to the polarizers (Figure S4, Supporting Information), indicating the anisotropic arrangement of CNCs in the films along the stretching direction. The interference color became more obvious with increasing CNCs contents from 1 to

3 wt% in original hydrogels (Figure 1c). The content of CNCs could only be enhanced to a certain value due to the aggregation of CNCs, generally less than 5 wt% CNCs (Figure S5, Supporting Information). Therefore, the concentration of 2 wt% CNCs in the dynamic hydrogels was chosen for the subsequent experiment. More importantly, the interference color was readily adjusted by changing the stretching ratios (ε) and width/thickness ratios (WTR) (Figure 1d,e). When ε increased from 8 to 16, the interference color of the composite films tuned from red to violet, showing the promoted alignment of CNCs in the films. Moreover, the interference color of the composite films changed gradually from red through blue/green to yellow with increasing WTR, indicating the weakened alignment of CNCs.[18]

In addition to the parameters during the preparation of dried composite films, we found that these single composite films could be stacked in piles with certain rotation angles to tune the light retardation and thus the interference colors. Thus, these films generally demonstrate as single modular components for further material design. As presented in **Figure 2**a, for the specific operation, these piled CNCs composite films showed vivid interference colors in broader ranges between the crossed polarizers (Figure 2b). To make sure that the films remain in the desired position, each film was fixed on glass slide that does not generate interference color. By increasing the stacking thickness from 0.12 to 1.08 mm, the piled CNCs films in the middle area showed clear and uniform interference colors, which changed within a much broad color range from gray-black through red and green to yellow green. The corresponding diagram of Commission International de L'Éclairage (CIE) chromaticity coordinates of obtained colors showed that a broad color range was achieved using piled CNCs composite films (Figure 2c). In addition, the corresponding UV–vis–NIR spectra were red-shifted with increasing stacking thickness (Figure S6, Supporting Information), which further proved the similar changes of the interference colors from gray-black to yellow green. These diverse interference colors were primarily because of modified light retardations, which are accumulated phase difference between light vibrating perpendicularly and parallel to the films containing aligned CNCs. Larger thickness of stacked CNCs composite films enhanced the light retardation due to the presence of more CNCs in the propagation pathway of light (Figure 2d). The light retardation can be described by the birefringence, which is generally quantified as the maximum difference between refractive indexes exhibited by anisotropic materials. In line with rising light retardation, the birefringence for the stacked CNCs films with larger thickness from 0.12 to 1.08 mm increased from 0.0005 to 0.001 (Figure 2d).

Moreover, the retardations of the piled CNCs films were almost the sum of those of the individual CNCs films (Table S1, Supporting Information). By changing the order of the piled CNCs composite films, the corresponding light retardation and birefringence only slightly changed (Table S2, Supporting Information). Consequently, the interference color nearly maintained for the same thickness of piled CNCs composite films independent on the order of stacking films (Figure S7, Supporting Information). This fact further confirms the critical role of the amount of CNCs in addition to the alignment of CNCs within the matrix in the propagation way of light, which predominantly affect the light retardation. To change the amount of CNCs in the light pathway and thus the retardation (Figure S8,
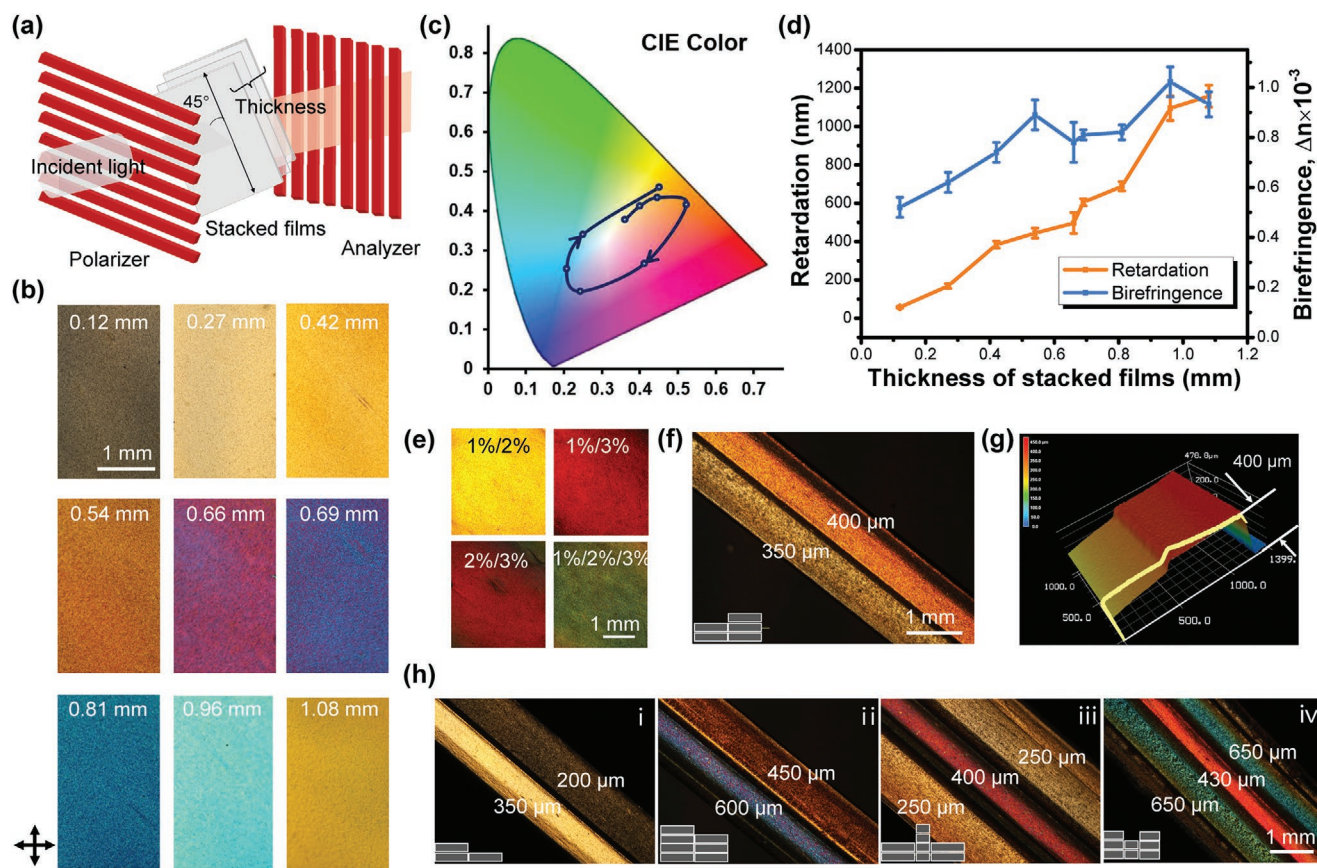
Figure 2. Interference color manipulation of the CNCs composite films piles via changing the thickness of the stacked films. a) Schematic illustration for the experimental setup of stacked CNCs composite films. b) Color evolution with the increasing thickness of the CNCs composite films pile from 0.12 to 1.08 mm. c) Color changes presented at a standard CIE-1931 color space. d) Light retardation and birefringence of CNCs composite films piles with various thicknesses. e) POM images of composite films piles with different CNCs concentrations. f) Patterned CNCs composite films with two colored strips fabricated from the hydrogel by controlling the thickness and width. The inset at the corner showed the cross sections of the initial 3D patterned hydrogel with the thicknesses of 2 and 3 mm and the width of 5 mm. g) 3D LSM image of the patterned CNCs composite film in (f). The inset shows the height profile of the patterned film. h) Patterned CNCs composite films with various thicknesses and widths. The insets show the cross section of the initial 3D patterned hydrogels with various thicknesses and widths. The numbers denote the thickness of the corresponding patterns of dried films.

Supporting Information), CNCs composite films with distinct amounts of CNCs can be used, which were derived from the different initial concentrations in the hydrogels. It is obvious that such piled composite films with equal thickness showed modified and tunable interference colors from orange to green (Figure 2e). This also provides another choice to change the amount of CNCs for the films with desired colors. Therefore, these single CNCs composite films can be modularly used by arbitrarily stacking them together to achieve desired light retardations and thus interference colors. A broad range of interference colors can be obtained by facilely combining these CNCs composite films, providing a simple and highly efficient approach for the photonic materials. As shown in Figure S9 (Supporting Information), the interference color of the uppercase letter "F" was easily tuned by increasing the layers of CNCs films under the crossed polarizers, which demonstrated the promising potential of such materials for energy-efficient displays, instead of using active light-emitting elements.[2]

Therefore, based on the fact that the interference colors can be manipulated by altering the amount of CNCs in the light pathway, we can prepare composite films containing patterned

regions showing diverse interference colors within one film (Figure 2f–h). These patterned regions with diverse thicknesses were prepared using patterned hydrogels containing regions with different thicknesses or widths (insets in Figure 2f–h). After stretching and air-drying, the CNCs composite films contained striped regions presenting distinct and vivid interference colors. For instance, Figure 2f illustrates such a patterned CNCs composite film originating from a patterned hydrogel containing stripes with different thicknesses of 2 and 3 mm but the same width of 5 mm. After stretching and air-drying, these two stripes generated distinct thicknesses of 350 and 400 µm, as measured using 3D LSM (Figure 2g), leading to totally different interference colors. Therefore, CNCs composite films with patterned multicolors were obtained by regulating the thickness and width of the integrated stripes within the initial patterned hydrogels (Figure 2h). In addition, the width of the stripes significantly affected the final interference colors, based on the effect of distinct WTR (Figure 1e). As displayed in Figure 2h-ii,iv, the stripes of the hydrogels with the same thickness (3 mm) but diverse widths of 5 and 3 mm showed totally different interference colors as orange and blue colors after

ADVANCED
SCIENCE NEWS
www.advancedsciencenews.com

ADVANCED
OPTICAL
MATERIALS
www.advopticalmat.de

stretching and air-drying, respectively. It should be noted that it is the first time to fabricate such patterned CNCs composite films with clear boundaries of distinct and uniform interference colors within one film starting with patterned hydrogels, which demonstrates an efficient and facile approach to prepare multicolor materials for potential applications in artificial intelligence and smart materials.[20,21]

In addition to adjusting the amount of CNCs by altering the total thickness of piled CNCs composite films, the relative organization of CNCs in the individual films can be tuned by stacking the films with certain rotation angles (**Figure 3**a). Here, two groups of piled CNCs composite films were selected to exhibit the distinct evolution of the interference colors, including one group of piled films with huge thickness difference and the other group of piled films with similar thickness.

As illustrated in Figure 3b with two CNCs films with significantly different thicknesses, the interference colors of piled films exhibited color development in a broad range depending on the rotation angles. While rotating the film B (0.395 mm) with fixed film A (0.244 mm) from 0° to 180°, the interference color of the stacked CNCs composite films between the crossed polarizers changed from fuchsia to light yellow and then turned back to fuchsia. Moreover, the light retardation of the stacked films is around 531 nm at 0°, which is almost the sum of those of the individual CNCs composite films (62 nm for film A and 418 nm for film B). Figure 3c further reveals a strong decrease of light retardation from 531 to 141 nm by increasing the rotation angle from 0 to 45°, and increased evidently with the rotation angle increasing to 90°. The corresponding birefringence also showed the same tendency. Besides, the light retardation and birefringence were almost symmetrical by the rotation
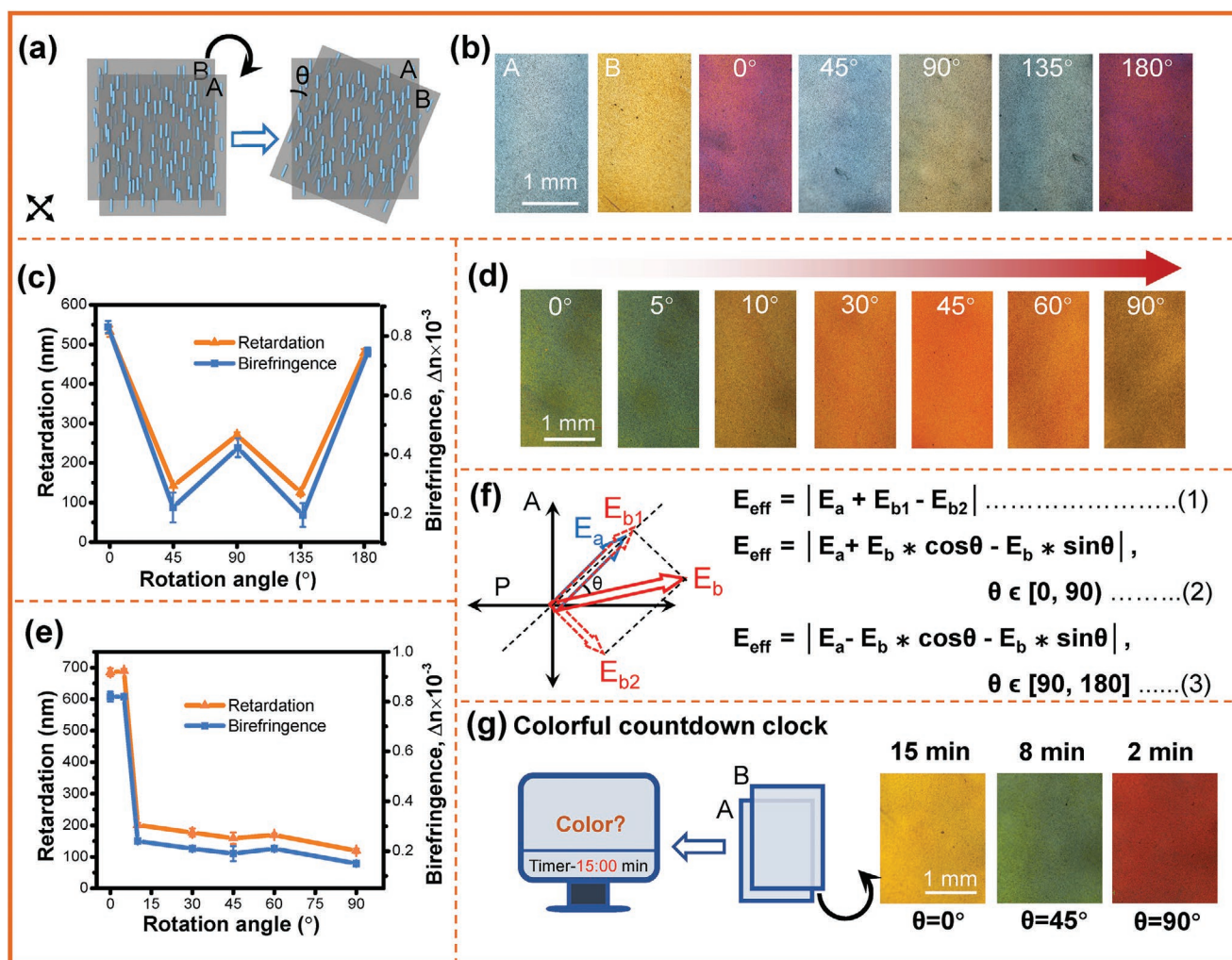

Figure 3. Interference color manipulation of piled CNCs composite films via changing the rotation angles. a) Schematic illustration of stacked CNCs composite films with rotation angles from 0° to 180°. b) Color evolution with increasing rotation angles of two stacked films with thickness of 0.244 mm (A) and 0.395 mm (B). c) Corresponding light retardation and birefringence of the stacked films in (b) with various rotation angles. d) Detailed color evolution of two stacked films with both thickness of 0.4 mm with the increasing rotation angle from 0° to 90°. e) Light retardation and birefringence of stacked CNCs composite films in (d) with rotation angles from 0° to 90°. f) Vector graphic illustration of the effect of rotation between two stacked CNCs composite films on the interference colors. E_{eff}: the effective alignment extent of the CNCs in the composite films at 45° against crossed polarizers. g) Demonstration of stacked CNCs films with changing rotation angles for the application as a colorful countdown clock. Scale bar: 1 mm.

**ADVANCED
SCIENCE NEWS**
www.advancedsciencenews.com

**ADVANCED
OPTICAL
MATERIALS**
www.advopticalmat.de

angle of 90°. Therefore, the development of the interference colors of piles films with the rotation angles between 0° and 90° should be the same as those of piles films with the rotation angles between 90° and 180°.

Another group of piled films using two single CNCs films with similar thickness of ≈0.4 mm showed more vivid and multiple colors from green through orange and finally to gray, while changing the rotation angles between 0° and 90° (Figure 3d). The interference colors turned back to green with steadily higher rotation angle from 90° to 180°, as demonstrated in the corresponding CIE in Figure S10 (Supporting Information). The light retardation of the CNCs films pile (383 nm for film A and 292 nm for film B) is around 694 nm at the rotation angle of lower than 5°. In comparison, the light retardation dramatically decreased to 150 nm, when the rotation angle was raised to 10°. This dramatic reduction of the light retardation and birefringence should be because of strongly reduced phase difference between light vibrating perpendicularly and parallel to aligned CNCs. Furthermore, the light retardation and birefringence further decreased with further enhancing rotating angle to 90°, which is different with the results in Figure 3c.

The effect of stacked CNCs films with diverse rotation angles can be schematically explained using the vectors showing the alignment extent of CNCs in the composite films as illustrated in Figure 3f. Given that the CNCs film showed the maximum intensity of the interference color with the stretching direction fixed at 45° against polarizers, the direction at 45° against polarizers was set as the baseline and the alignment extent of CNCs in the films along this baseline was defined as the effective alignment extent (E_{eff}). Stacking more CNCs films with the orientation of CNCs in this direction will enhance the alignment extent that is presented as the sum of the extents derived from individual films (Figure S11a, Supporting Information). Therefore, the retardation and birefringence increased with the increasing stacking thickness (Figure 2d). On the other hand, by rotating one CNCs composite film (b) from the baseline to a specific rotation angle (θ), the alignment extent of film b (E_b) could be separated into two crossed alignment extents (E_{b1} and E_{b2}), which were parallel or perpendicular to the baseline, respectively (Figure 3f). Consequently, the effective alignment extent (E_{eff}) of two stacked films referring to baseline will be

$$E_{eff} = |E_a + E_{b1} - E_{b2}| \tag{1}$$

Due to the presence of diverse rotation angles (θ), formula (1) can be expressed with two specific forms as shown in formulas (2) and (3) (Figure 3f)

$$E_{eff} = |E_a + E_b \cdot \cos\theta - E_b \cdot \sin\theta|, \quad \theta \in [0, 90°) \tag{2}$$

$$E_{eff} = |E_a - E_b \cdot \cos\theta - E_b \cdot \sin\theta|, \quad \theta \in [90°, 180°] \tag{3}$$

Based on these formulas, a few specific situations can be explained (Figure S11, Supporting Information). For instance, rotating film b to the rotation angle of 45° or 135°, the effective alignment extent (E_{eff}) of the pile will be only E_a (Figure S11b, Supporting Information). Therefore, the interference color of the pile at the rotation angle of 45° and 135° was the same as the interference color of film a (Figure 3b). In a similar manner, rotating film a to the rotation angle of 45° or 135°, the interference color of the piles will only be the interference color of film b, as demonstrated in Figure S12 (Supporting Information). Moreover, E_{eff} at the rotation angle of 90° is the difference between E_a and E_b, which is however highly dependent on their relative light retardation (Figure S11c,d, Supporting Information). When E_a was much lower than E_b, E_{eff} at 90° will be much higher than that at 45°, producing higher light retardation as proved in Figure 3c. Otherwise, E_{eff} at 90° will be the lowest resulting in the lowest light retardation (Figure 3e). Therefore, rotating one CNCs composite film of the piled films to regulate the arrangement of CNCs can be used to adjust the interference color in a facile manner with the great upscaling potential, and the organization of the individual CNCs film also plays an important role for the final interference colors of the piled films with certain rotation angle. The direct visualization can be applied in many fields, such as sport, parking, catering, and other service industry. For instance, the piled CNCs films can be used as countdown clock for visualization (Figure 3g). By regulating the rotation angles of the film "B," yellow, green and red color were obtained to represent remaining 15, 8, and 2 min, respectively.

Being able to arbitrarily control the interference colors of the CNCs composite films as modular components by altering the pile thickness and rotation angle, we developed an optical security system based on the patterned CNCs films (Figures 2f–h and 4). In the accounting system, the binary-coded decimal (BCD) is a system of writing numerals that assigns a four-digit binary code to each digit of 0 to 9 in a decimal numeral.[22] Similar as BCD, we developed a ternary-coded decimal system using our piled CNCs composite films with three individual interference colors (black, gray, and orange referred to as digit 0, 1 and 2, respectively).

Ten four-digit ternary codes, represented by the four colorful squares, can be defined as each decimal numeral of 0–9, as illustrated in Figure 4a. The four colorful squares can be realized by stacking and rotating the CNCs composite piles, as proved in Figure 4b. By stacking two patterned CNCs composite films with the rotation angle of 90°, the square patterns with the three individual colors were obtained due to diverse alignment extents of CNCs. Due to the presence of two patterns in each CNCs composite film, piled films formed two intersections with four squares. The corresponding POM images of the two intersections exhibited distinct and specific interference colors in each square due to diverse alignment extents (Figure S13a,b, Supporting Information).

These patterned CNCs composite films can be further used as modular components to achieve various square patterns by simply combining the CNCs composite films (Figure S13c,e, Supporting Information). It is also obvious that the squares with the same piled films generated equal interference color. Therefore, those ten patterned CNCs films piles are used as the fundamental building blocks for the decimal numerals for further programming. The numbers can be directly read according to the colors of the CNCs film piles. For instance, the combination of two colorful squares in Figure 4c can be translated into two numerals 6 and 4, leading to the number 64. By freely combining the fundamental elements, more complex information can be encoded (Figure 4d). Moreover, every number can
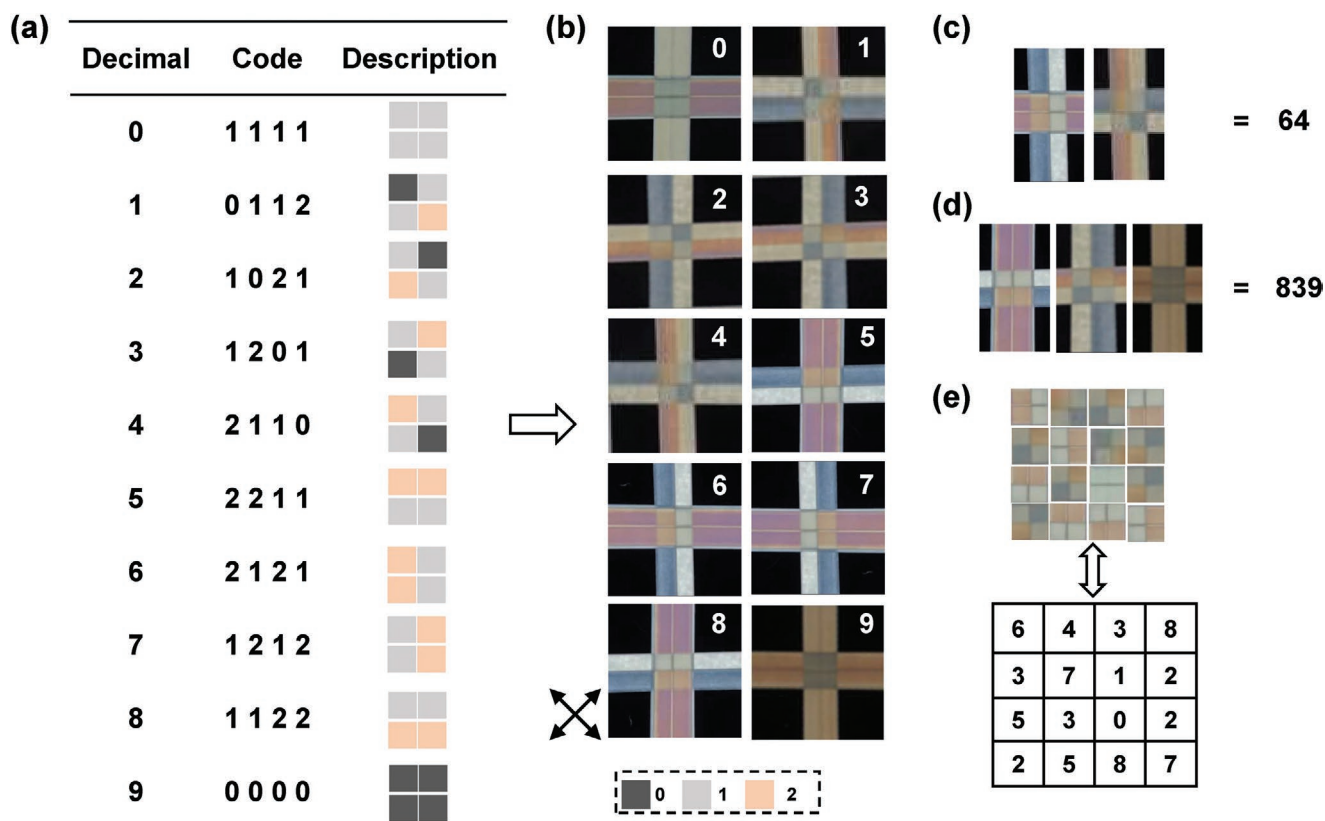
Figure 4. Ternary-coded decimals using patterned CNCs composite films. a) Encryption system for translating ternary code represented by colorful squares with three colors into decimal. b) Ten fundamental elements made by piles of patterned CNCs composite films between the crossed polarizers representing 0–9 in decimal. c,d) Reading-out process according to the colors of CNCs film piles. e) A 3D QR code for the information storage and encryption via the combination of the fundamental elements.

be encrypted by combining these fundamental building blocks and the data pool can also be simply enlarged by incorporating more patterns with more color combinations.

Based on this ternary numeral system, the building blocks of CNCs film piles encoding 0–9 were used to construct a 3D QR code, which contain the desired digital information (Figure 4d). Compared with the traditional QR code with two interference colors of black and white, 3D QR codes with various colors are much more precise and secure. Importantly, the fundamental building blocks can be endowed with more interference colors by changing the WTR, ε, and thickness of the patterned CNCs composite films, which will further improve the capacity of coding system. Therefore, such ternary-coded decimal systems with distinguishable and exactly programmable colors show big potential in information transfer or encryption fields.[21,23] To our best of knowledge, this is also the first example to use patterned CNCs composite film with uniform and tunable interference colors for precise and effective security system and encryption.

In summary, we found that composite films with organized CNCs showing uniform and tunable interference colors can be used for precise and effective security system and encryption. We developed a novel facile method by piling CNCs composite films to alter the amount of CNCs in the propagation pathway of light or by altering the rotation angles between the individual films to change the relative organization of CNCs. In particular,

a broad color range was achieved by using CNCs composite films with diverse thicknesses and concentrations of CNCs as modular components, and the interference colors were also tunable by changing the rotation angles between individual CNCs composite films. This simple but efficient new method provides an alternative way for the development of optical materials by only modifying the relative organization of CNCs in the propagation pathway of light in addition to existing methods, such as those based on photonic crystals. These CNCs composite films with tunable interference colors can be applied for various fields, such as optical encryption, and pave the way of using anisotropic nanostructures for photonic functional materials including optical coding.

Supporting Information

Supporting Information is available from the Wiley Online Library or from the author.

Acknowledgements

**ADVANCED
SCIENCE NEWS**

www.advancedsciencenews.com

**ADVANCED
OPTICAL
MATERIALS**

www.advopticalmat.de

Conflict of Interest

The authors declare no conflict of interest.

Keywords

cellulose nanocrystals, encryption, interference colors, nanocomposites, photonic materials

[1] T. D. Nguyen, W. Y. Hamad, M. J. MacLachlan, *Chem. Commun.* **2013**, *49*, 11296.

[2] W. Fan, J. Zeng, Q. Q. Gan, D. X. Ji, H. M. Song, W. Z. Liu, L. Shi, L. M. Wu, *Sci. Adv.* **2019**, *5*, eaaw8755.

[3] a) Y. Wang, H. Cui, Q. Zhao, X. Du, *Matter* **2019**, *1*, 626; b) T. Hiratani, W. Y. Hamad, M. J. MacLachlan, *Adv. Mater.* **2017**, *29*, 1606083; c) J. Y. Chen, L. R. Xu, X. F. Lin, R. L. Chen, D. Yu, W. Hong, Z. K. Zheng, X. D. Chen, *J. Mater. Chem. C* **2018**, *6*, 7767; d) H. Z. Zheng, W. R. Li, W. Li, X. J. Wang, Z. Y. Tang, S. X. A. Zhang, Y. Xu, *Adv. Mater.* **2018**, *30*, 1705948.

[4] J. A. Kelly, A. M. Shukaliak, C. C. Y. Cheung, K. E. Shopsowitz, W. Y. Hamad, M. J. MacLachlan, *Angew. Chem., Int. Ed.* **2013**, *52*, 8912.

[5] G. Isapour, M. Lattuada, *Adv. Mater.* **2018**, *30*, 1707069.

[6] M. Giese, L. K. Blusch, M. K. Khan, M. J. MacLachlan, *Angew. Chem., Int. Ed.* **2015**, *54*, 2888.

[7] a) G. Siqueira, D. Kokkinis, R. Libanori, M. K. Hausmann, A. S. Gladman, A. Neels, P. Tingaut, T. Zimmermann, J. A. Lewis, A. R. Studart, *Adv. Funct. Mater.* **2017**, *27*, 1604619; b) R. M. Parker, G. Guidetti, C. A. Williams, T. Zhao, A. Narkevicius, S. Vignolini, B. Frka-Petesic, *Adv. Mater.* **2018**, *30*, 1704477; c) M. Mashkour, T. Kimura, M. Mashkour, F. Kimura, M. Tajvidi, *ACS Appl. Mater. Interfaces* **2019**, *11*, 1538; d) A. P. C. Almeida, J. P. Canejo,

S. N. Fernandes, C. Echeverria, P. L. Almeida, M. H. Godinho, *Adv. Mater.* **2018**, *30*, 1703655; e) K. J. De France, T. Hoare, E. D. Cranston, *Chem. Mater.* **2017**, *29*, 4609; f) Y. Habibi, L. A. Lucia, O. J. Rojas, *Chem. Rev.* **2010**, *110*, 3479; g) J. P. F. Lagerwall, C. Schutz, M. Salajkova, J. Noh, J. H. Park, G. Scalia, L. Bergstrom, *NPG Asia Mater.* **2014**, *6*, e80; h) K. E. Shopsowitz, H. Qi, W. Y. Hamad, M. J. Maclachlan, *Nature* **2010**, *468*, 422.

[8] O. Kose, A. Tran, L. Lewis, W. Y. Hamad, M. J. MacLachlan, *Nat. Commun.* **2019**, *10*, 510.

[9] Q. Chen, P. Liu, F. C. Nan, L. J. Zhou, J. M. Zhang, *Biomacromolecules* **2014**, *15*, 4343.

[10] B. Frka-Petesic, G. Guidetti, G. Kamita, S. Vignolini, *Adv. Mater.* **2017**, *29*, 1701469.

[11] K. Yao, Q. Meng, V. Bulone, Q. Zhou, *Adv. Mater.* **2017**, *29*, 1701323.

[12] a) B. Frka-Petesic, H. Radavidson, B. Jean, L. Heux, *Adv. Mater.* **2017**, *29*, 1606208; b) J. H. Park, J. Noh, C. Schutz, G. Salazar-Alvarez, G. Scalia, L. Bergstrom, J. P. F. Lagerwall, *ChemPhysChem* **2014**, *15*, 1477.

[13] S. Beck, J. Bouchard, G. Chauve, R. Berry, *Cellulose* **2013**, *20*, 1401.

[14] A. Tran, W. Y. Hamad, M. J. MacLachlan, *ACS Appl. Nano Mater.* **2018**, *1*, 3098.

[15] Y. L. Zhou, Y. Y. Li, F. Dundar, K. R. Carter, J. J. Watkins, *Cellulose* **2018**, *25*, 5185.

[16] a) H. Wan, X. F. Li, L. Zhang, X. P. Li, P. F. Liu, Z. G. Jiang, Z. Z. Yu, *ACS Appl. Mater. Interfaces* **2018**, *10*, 5918; b) M. K. Khan, A. Bsoul, K. Walus, W. Y. Hamad, M. J. MacLachlan, *Angew. Chem.* **2015**, *127*, 4378; *Angew. Chem., Int. Ed.* **2015**, *54*, 4304; c) Y. Zhang, Z. J. Tian, Y. J. Fu, Z. J. Wang, M. H. Qin, Z. W. Yuan, *Carbohydr. Polym.* **2020**, *228*, 115387.

[17] C. Boott, A. Tran, W. Hamad, M. MacLachlan, *Angew. Chem.* **2020**, *132*, 232; *Angew. Chem., Int. Ed.* **2020**, *59*, 226.

[18] H. Q. Huang, X. J. Wang, J. C. Yu, Y. Chen, H. Ji, Y. M. Zhang, F. Rehfeldt, Y. Wang, K. Zhang, *ACS Nano* **2019**, *13*, 3867.

[19] a) R. Kizhakidathazhath, Y. Geng, V. S. R. Jampani, C. Charni, A. Sharma, J. P. F. Lagerwall, *Adv. Funct. Mater.* **2020**, *30*, 1909537; b) Y. Mao, E. M. Terentjev, M. Warner, *Phys. Rev. E* **2001**, *64*, 041803.

[20] J. Zou, S. Q. Wu, J. Chen, X. J. Lei, Q. H. Li, H. Yu, S. Tang, D. D. Ye, *Adv. Mater.* **2019**, *31*, 1904762.

[21] Z. Zhao, H. Wang, L. R. Shang, Y. R. Yu, F. F. Fu, Y. J. Zhao, Z. Z. Gu, *Adv. Mater.* **2017**, *29*, 1704569.

[22] a) A. K. Biswas, M. Hasan, A. R. Chowdhury, H. M. H. Babu, *Microelectron. J.* **2008**, *39*, 1693; b) M. M. Panahi, O. Hashemipour, K. Navi, *Integration* **2018**, *62*, 353.

[23] M. L. You, M. Lin, S. R. Wang, X. M. Wang, G. Zhang, Y. Hong, Y. Q. Dong, G. R. Jin, F. Xu, *Nanoscale* **2016**, *8*, 10096.